

**PSFC/JA-01-24**

**Beta Limiting MHD Activity and Mode Locking  
in Alcator C-Mod**

J.A. Snipes, R.S. Granetz, R.J. Hastie, A.E. Hubbard, Y. In,  
D. Mossessian, J.E. Rice, J.J. Ramos, D. Schmittiel,  
G. Taylor<sup>1</sup>, S.M. Wolfe

October 2001

Plasma Science and Fusion Center  
Massachusetts Institute of Technology  
Cambridge, MA 02139 USA

<sup>1</sup>Princeton Plasma Physics Laboratory, Princeton, NJ 08543.

This work was supported by the U.S. Department of Energy, Cooperative Grant No. DE-FC02-99ER54512. Reproduction, translation, publication, use and disposal, in whole or in part, by or for the United States government is permitted.

Submitted for publication to *Plasma Physics and Controlled Fusion*.

## Beta Limiting MHD Activity and Mode Locking in Alcator C-Mod

J A Snipes, R S Granetz, R J Hastie, A E Hubbard, Y In, D Mossessian, J E Rice,  
J J Ramos, D Schmittdiel, G Taylor\*, S M Wolfe

MIT Plasma Science and Fusion Center, Cambridge, MA 02139, USA  
\*Princeton Plasma Physics Laboratory, Princeton, NJ 08543

**Abstract** When operating at low collisionality and high input power ( $P_{\text{ICRF}} \leq 5$  MW), large amplitude ( $5 \times 10^{-5} < [\tilde{B}_\theta / B_\theta]_{\text{wall}} \leq 5 \times 10^{-3}$ ) low frequency ( $f_{\text{MHD}} < 50$  kHz) MHD modes appear to limit the achievable  $\beta$  in Alcator C-Mod. Modes with  $m/n = 5/4, 4/3, 3/2,$  and  $2/1$  were destabilized when  $\beta_p > 0.52$  and increased in amplitude with increasing  $\beta$  until a rollover or collapse in  $\beta$  occurred. The largest amplitude modes with  $m=2, n=1$  strongly degraded momentum and energy confinement when the modes coupled across the plasma core and locked to the wall, bringing the plasma ion toroidal rotation to zero, within experimental errors, about 50 ms after mode locking. MHD stability was calculated with the MARS code for a discharge with a large  $m=2, n=1$  mode. Comparisons were made with Neoclassical Tearing Mode (NTM) theory and with NTM's found on other tokamaks.

### 1. Introduction

With high power ICRF heating ( $P_{\text{RF}} \leq 5$  MW) on Alcator C-Mod, high performance plasmas are readily obtained with normalized beta values,  $\beta_N = \beta_T / (I/aB_T)$ , exceeding 1.2 and maximum values as high as 1.7 in H-mode. The toroidal and poloidal  $\beta$  parameters are the usual ratios of the average plasma kinetic pressure to the magnetic pressure,  $\beta_T = 2\mu_0 \langle p \rangle / B_T^2$  and  $\beta_p = 2\mu_0 \langle p \rangle / B_\theta^2$ . All of the 2000 campaign discharges with  $\beta_N > 1.2$  were analysed for low frequency ( $f_{\text{MHD}} < 50$  kHz) MHD activity associated with high  $\beta$ . At high density ( $\bar{n}_e > 2.5 \times 10^{20} \text{ m}^{-3}$ ) and high collisionality,  $v_{q=2} = [v_i / (\epsilon\omega_*e)]_{q=2} \geq 1$ , sawtooth precursors and small ELMs dominate the MHD activity with rapid chaotic spikes on top of an Enhanced  $D_\alpha$  H-mode (EDA) [1]. At lower collisionality,  $v_{q=2} \leq 0.5$ , a small number of discharges in ELM-free H-mode had moderate to large amplitude MHD modes ( $5 \times 10^{-5} < [\tilde{B}_\theta / B_\theta]_{\text{wall}} \leq 5 \times 10^{-3}$ ) with  $m/n = 2/1, 3/2, 4/3,$  and  $5/4$ , which were destabilized at  $\beta_p > 0.52$  and increased in amplitude with increasing  $\beta$  until a rollover or collapse in  $\beta$  occurred.

The largest amplitude modes had  $m=2, n=1$  and strongly degraded both momentum and energy confinement when the modes coupled across the core of the plasma to an  $m=1, n=1$  mode (Figure 1). The core toroidal plasma rotation dropped to zero, within experimental errors, about 50 ms after the modes locked to the wall, indicating a momentum confinement time that is somewhat longer than the energy confinement time ( $\tau_E \approx 33$  ms). Because of the correlation with low collisionality and high  $\beta$ , comparisons were made with neoclassical tearing mode (NTM) theory [2-5] and with similar modes found on other tokamaks [4-9].

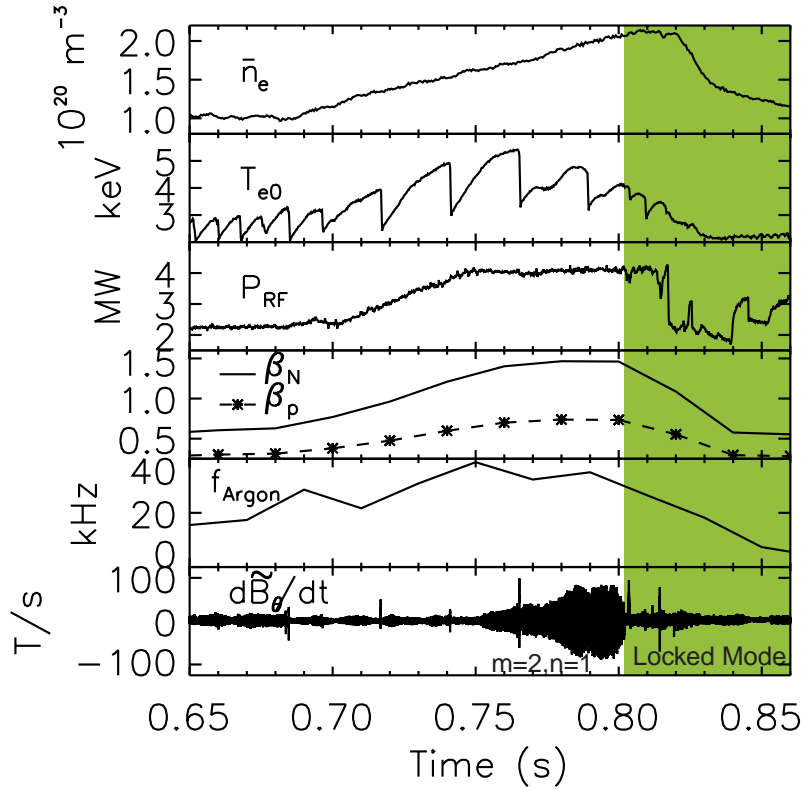


**Figure 1** A high  $\beta$  discharge with a large  $m=2, n=1$  mode that leads to a  $\beta$  collapse. The line averaged density, central  $T_e$ , ICRF power,  $\beta_N$ ,  $\beta_p$ , toroidal ion rotation frequency, and  $d\tilde{B}_\theta/dt$  are shown. The shaded region is during the locked mode.

Calculations were done with the MARS code [10] together with separate numerical calculations to determine the MHD stability properties of a discharge with a large  $m=2, n=1$  mode.

## 2. Experimental conditions

Alcator C-Mod is a compact high field ( $B_T \leq 8$  T) divertor tokamak [11] with a major radius of 0.67 m, a minor radius of 0.22 m and a typical elongation of 1.7. In these experiments, hydrogen minority Ion Cyclotron Range of Frequency (ICRF) heating at 78 – 80 MHz was used at an on-axis field of  $B_T = 5.4$  T to provide central resonance heating with plasma currents of 0.8 – 1.0 MA. One 4-strap and two 2-strap ICRF antennas are each driven with  $0-\pi$  phasing so that there is no net current drive or direct momentum input.

The main diagnostics used in this paper include a poloidal array of 15 and a toroidal array of 5 poloidal field pick-up coils (Figure 2), a 9 channel Electron Cyclotron Emission (ECE) Grating Polychromator [12], and a spatially fixed von Hamos type crystal x ray spectrometer [13-14]. The pick-up coils are sampled at 1 MHz with unequal poloidal and

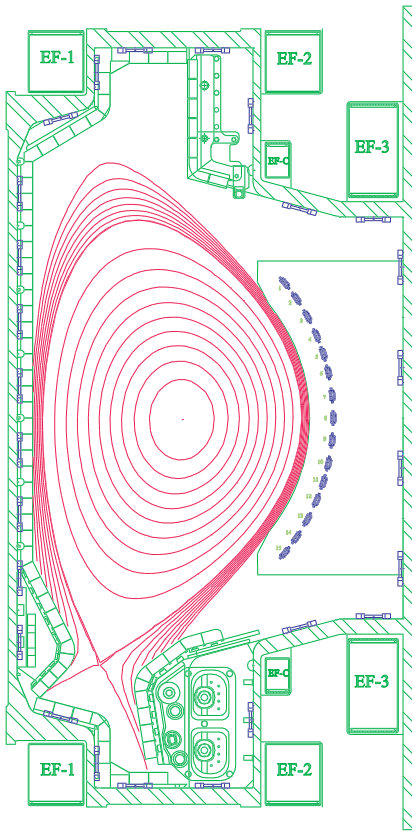


**Figure 2.** A cross-section of Alcator C-Mod showing in dark blue the magnetic pick-up coils at one toroidal location.

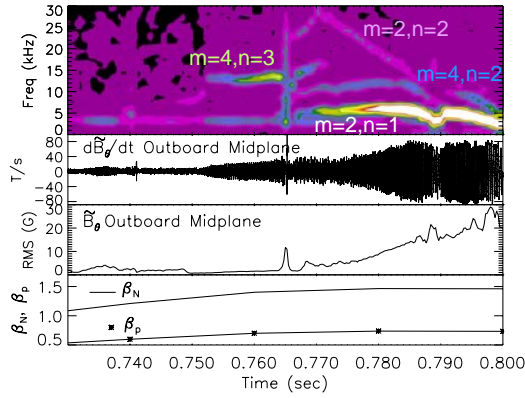
collisionality with  $\nu_{q=2} < 0.5$ . Two discharges had similar very large  $m=2, n=1$  modes with  $[\tilde{B}_\theta / B_\theta]_{\text{wall}} \approx 5 \times 10^{-3}$  preceded by smaller amplitude  $m=4, n=3$  modes (Figure 3a). Two other discharges had similar cascades of  $m=5, n=4$  then  $m=4, n=3$  modes with moderate amplitudes of  $[\tilde{B}_\theta / B_\theta]_{\text{wall}} \approx 5 \times 10^{-5}$  (Figure 3b). One discharge had an intermediate amplitude ( $[\tilde{B}_\theta / B_\theta]_{\text{wall}} \approx 2.5 \times 10^{-4}$ )  $m=3, n=2$  mode (Figure 3c). Figure 3 shows the auto-power spectrum of an outboard midplane pick-up coil signal together with the RMS poloidal field mode amplitude at the wall and the poloidal and normalized toroidal  $\beta$  time traces. All of the discharges had sawteeth, whose associated modes are visible as regular spikes in the mode amplitude, which may provide seed islands for NTM's.

In the cases of the very large  $m=2, n=1$  modes (Figure 3a), the discharges were in ELM-free H-mode with  $I_p = 1$  MA,  $B_T = 5.4$  T,  $q_{95} \approx 4$ , and  $\nu_{q=2} \approx 0.1 - 0.2$ . The mode amplitude increased with increasing  $\beta_p$ , suggestive of NTM's, then the frequency slowed down and the mode locked. The confinement degraded substantially after the mode locked,

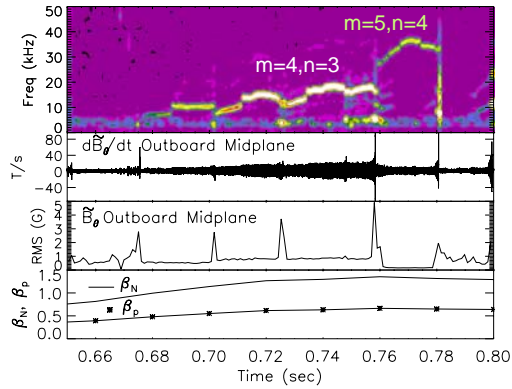
toroidal spacing. The ECE channels are sampled at 20 kHz and have a radial spacing of about 2 cm. The x ray crystal spectrometer has a line of sight tangent to the plasma axis. It measures the toroidal ion rotation velocity from Doppler shifts of  $\text{Ar}^{17+}$  emission, which comes from the hot core region of the plasma, with 20 ms time resolution. Trace argon impurities are added to the plasma to make these measurements. The uncertainty in the argon ion rotation frequency depends on the argon signal level but is typically  $\sim 2$  kHz. For comparison, the magnetic pick-up coil data can be fast Fourier transformed at 1 ms intervals with 1 kHz frequency resolution.

### 3. MHD mode analysis at high $\beta$

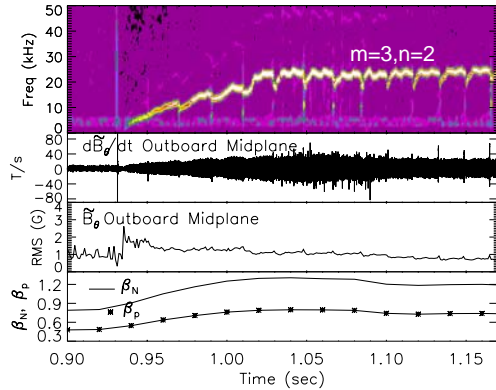
Moderate to large amplitude modes that appear to limit the maximum  $\beta_N$  achievable were found in only five of the high beta discharges analyzed. All five of these discharges had relatively low



(a)



(b)



(c)

**Figure 3.** The auto-power spectra of a pick-up coil signal showing (a) a large  $m=2, n=1$  mode, (b) a cascade of  $m=4, n=3$  and  $m=5, n=4$  modes, and (c) an  $m=3, n=2$  mode together with the RMS poloidal field mode amplitude and  $\beta_N$  and  $\beta_p$ . Brighter color means higher amplitude.

which then reduced  $\beta$  (Figure 1). Due to equilibrium changes, the mode amplitude cannot be determined accurately while the mode is locked, but the small irregular sawteeth, near zero plasma rotation velocity, and poor confinement throughout the remainder of the discharge indicate a substantial locked mode remains until the plasma disrupts more than 0.7 s later. An NTM would be expected to decrease sharply in amplitude with decreased  $\beta$ , so this suggests that these are more likely to be resistive tearing modes or may be error field induced modes [15].

The discharges with smaller amplitude cascades of  $m=4, n=3$  and  $m=5, n=4$  modes at high  $\beta$  (Figure 3b) were in ELM-free H-mode and had  $P_{ICRF} = 2.5$  MW,  $I_p = 0.8 - 1$  MA,  $B_T = 5.4$  T,  $q_{95} \approx 3.9 - 4.8$ ,  $\beta_N \approx 1.35 - 1.5$ ,  $\bar{n}_e \approx 2 \times 10^{20} \text{ m}^{-3}$ , and  $v_{q=2} \approx 0.09 - 0.13$ . The higher order modes in these discharges are unusual in that a mode from such a deep rational  $q$  surface is not normally observed as the dominant mode with pick-up coils at the wall as it is usually coupled to a larger rational  $q$  surface that is closer to the pick-up coils. The sawtooth precursors provide large magnetic perturbations and these higher order modes appear to be driven unstable by the sawtooth collapse. In these cases, however, the  $m=4, n=3$  and  $m=5, n=4$  mode amplitudes do not exceed  $[\tilde{B}_\theta / B_\theta]_{\text{wall}}$

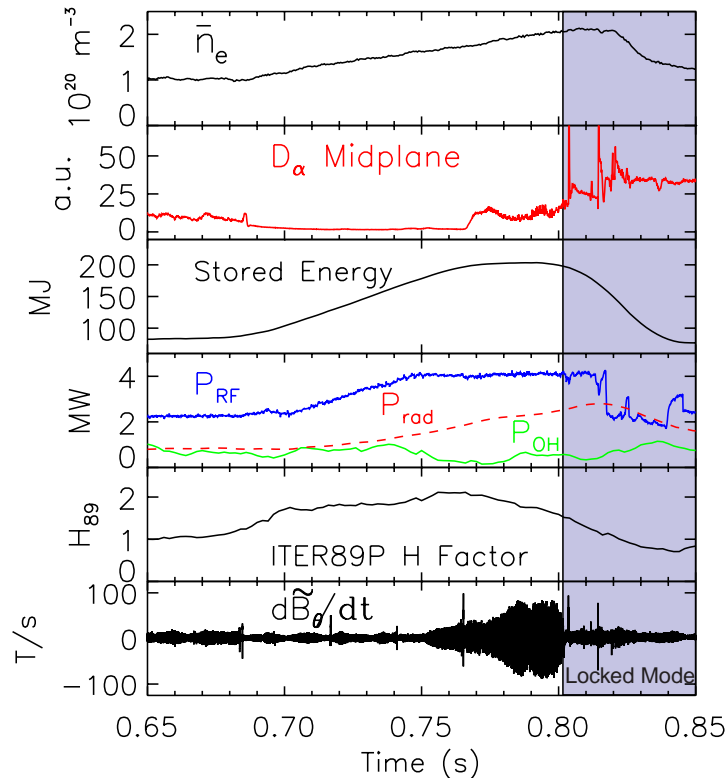


**Figure 4.** The line averaged density,  $D_\alpha$  emission, plasma stored energy, ICRF source power, total radiated power, Ohmic input power, H factor, and outboard midplane magnetic pick-up coil signal are shown for the discharge in Figure 1. The mode is locked during the shaded region.

$\leq 2.6 \times 10^{-4}$ , which indicates that they do not have the strong nonlinear drive characteristic of NTM's.

The  $m=3$ ,  $n=2$  mode in Figure 3c also appears to be triggered by a large sawtooth, but at relatively low  $\beta_N \approx 0.9$ . This discharge was in EDA H-mode and had  $I_p = 0.8$  MA,  $B_T = 5.4$  T,  $q_{95} = 4.6 - 5.1$ , and  $v_{q=2} \approx 0.52$ . The sawtooth collapse triggers the mode and then the L-H transition and the mode persists across the L-H transition and throughout the H-mode. Sauter has shown that NTM's can be destabilized on JET even at such low beta values if the seed island is sufficiently large [16]. While the mode frequency spins up with increasing  $\beta$ , the amplitude does not increase with  $\beta$ , which, together with the relatively high collisionality, suggests resistive tearing modes rather than NTM's.

#### 4. Momentum and energy confinement degradation

In the discharges with very large  $m=2$ ,  $n=1$  modes, both momentum and energy confinement were strongly degraded by the modes, as shown in Figures 1 and 4. The core ion toroidal rotation can be compared to the mode rotation frequencies together with the apparent mode

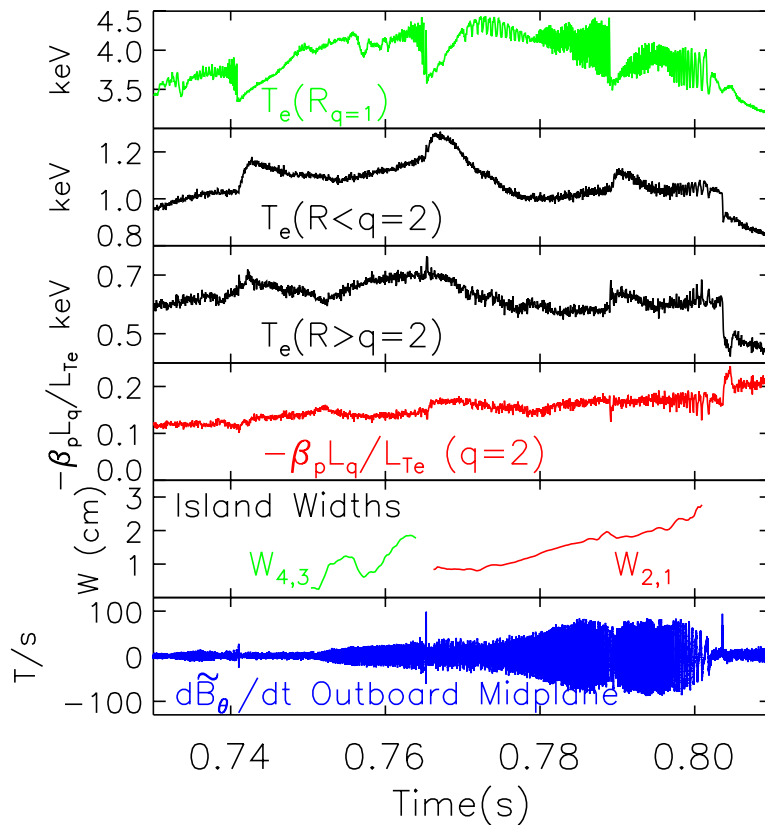


**Figure 5.** ECE  $T_e$  signals at the  $q=1$  and straddling the  $q=2$  surface and the bootstrap parameter  $-\beta_p L_q / L_{Te}$  at  $q=2$  showing an increase by about a factor of 2 as the  $m=4, n=3$  and  $m=2, n=1$  islands grow.

coupling across the plasma by also comparing magnetic modes measured at the edge with electron temperature oscillations on the core ECE channels. The drop in plasma stored energy has also been compared with that expected by the Chang and Callen belt model [17].

Figure 1 shows the core toroidal plasma ion rotation frequency was about 30 kHz at 0.77 s and began decreasing just as the mode locks at 0.8 s. The dominant magnetic mode frequency does not track the plasma rotation as it usually does [18] but is substantially slower, indicating a weak coupling of the sawtooth precursors to the modes near the edge of the plasma. Both the mode rotation and the plasma rotation are in the ion diamagnetic drift direction. The mode at 0.76 s with a frequency of about 14 kHz is predominantly an  $m=4, n=3$  mode (Figure 3a). After the next sawtooth crash, there is a faint mode with  $m=2, n=2$  that peaks at 28 kHz after the crash, which is close to the core ion rotation frequency at that time. Ion toroidal rotation velocity profiles were not measured in this shot, but in C-Mod they generally fall off quite rapidly with radius [19] so that already at the  $q=1$  surface, 10 cm from the center, the plasma rotation may be as low as 14 kHz to explain an  $n=2$  mode at twice that

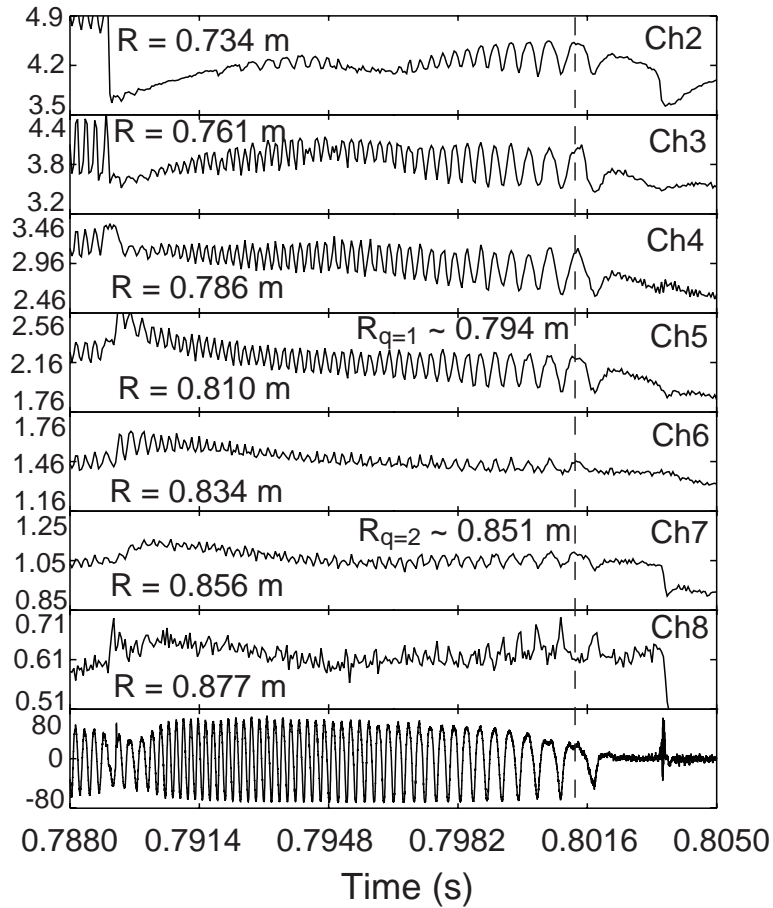


**Figure 6.** ECE  $T_e$  signals from the center to the edge showing no phase inversion across the  $q=1$  surface and a phase inversion between channels 7 and 8, near  $q=2$ , together with a magnetic pick-up coil signal

frequency. This  $n=2$  mode quickly slows down before the next sawtooth crash even though the core plasma is still rotating rapidly (Figure 1). During this phase from 0.766 s onward, the magnetic pick-up coil signals are dominated by a growing  $m=2$ ,  $n=1$  mode starting at 5 kHz and slowing down to lock at 0.802 s. A coupled  $m=4$ ,  $n=2$  harmonic is also present at twice the  $n=1$  mode frequency.

At 0.77 s, a low frequency oscillation appears on the 20 kHz sampled ECE signals near the  $q=1$  surface that is not coupled to the edge  $m=2$ ,  $n=1$  mode (Figure 5). Just before 0.78 s, when the  $m=2$ ,  $n=1$  amplitude exceeds  $[\tilde{B}_\theta / B_\theta]_{\text{wall}} \approx 1.9 \times 10^{-3}$ , the core mode frequency becomes the same as the  $m=2$ ,  $n=1$  frequency indicating strong coupling between the two modes. Despite the fact that the core plasma ions are still rotating at  $\sim 30$  kHz when the mode begins to lock, the  $m=1$ ,  $n=1$  mode in the core rotates with the much slower  $m=2$ ,  $n=1$  mode frequency and also locks at the same time (Figure 6). Once the  $m=2$ ,  $n=1$  mode couples strongly to the core  $m=1$ ,  $n=1$  mode, the core plasma rotation also begins to slow



down and it stops rotating at about 0.85 s (Figure 1). This indicates that the momentum confinement time is  $\sim 50$  ms, which is somewhat larger than the energy confinement time of  $\sim 33$  ms just after mode locking. Similar locking of core rotation to an  $m=2, n=1$  mode has been observed on JET [20].

When the  $m=2, n=1$  mode couples strongly to the core  $m=1, n=1$  mode, the energy confinement is seriously degraded (Figure 4). The H factor during the mode, relative to the ITER89P scaling [21], falls from  $H_{89} \sim 2.0$  to 0.7 despite 4 MW of ICRF heating, which is normally more than sufficient to keep the plasma above the H-mode threshold for similar conditions without the large  $m=2, n=1$  mode. The confinement continues to decrease with increasing mode amplitude. The stored energy saturates at the start of the oscillating  $m=2, n=1$  mode and then decreases rapidly when the mode locks just after 0.8 s. Then at 0.814 s, the ICRF power drops suddenly and the plasma reverts to L-mode.

The confinement degradation before the H-L transition can be compared to the Chang and Callen belt model for the change in stored energy due to large MHD islands [17]. For a given island, the drop in stored energy is predicted to be proportional to the island width according to:

$$\Delta W = 4P_{in} \tau_{inc0} r_s^3 \frac{W_{is}}{a^4} (0.32 + 0.39 \frac{a^2}{r_s^2}), \quad (1)$$

where  $P_{in}$  is the input power,  $\tau_{inc0} = \Delta W / \Delta P_{in}$  is the incremental energy confinement time,  $r_s$  is the radius of the mode rational surface,  $W_{is}$  is the island width, and  $a$  is the plasma minor radius. There was a ramp in ICRF power early in the discharge in Figure 4 that allows  $\tau_{inc0}$  to be determined and it is found to be about 47 ms at that time. The  $m=2, n=1$  island width is determined from a simple cylindrical expression for a tearing mode [22]:

$$W_{is} = 4r_s \sqrt{\frac{\tilde{B}_r q_s}{m B_\theta r_s' q_s'}}, \quad (2)$$

where all quantities are evaluated at the mode rational surface and  $\tilde{B}_r$  is the radial field perturbation due to the mode with poloidal mode number  $m$ ,  $B_\theta$  is the equilibrium poloidal field, and the prime denotes the radial derivative of the safety factor profile,  $q_s$ . The radial field perturbation at the resonant surface is related to the poloidal field perturbation measured at the wall by  $\tilde{B}_r|_{q=2} = \alpha (\frac{r_{coil}}{r_s})^{m+1} \tilde{B}_\theta|_{wall}$ . The extra factor,  $\alpha \approx 0.5$  for  $m=2, n=1$ , beyond a simple cylindrical current-free model comes about by integrating the MHD equation [23]:

$$r \frac{d}{dr} r \frac{d\tilde{\psi}}{dr} - m^2 \tilde{\psi} - \frac{q}{1 - nq/m} r \frac{d}{dr} \left( \frac{1}{r} \frac{d}{dr} r^2 \frac{d\tilde{\psi}}{dr} \right) = 0, \quad (3)$$

where  $\tilde{\psi}$  is the perturbed poloidal magnetic flux, solving for  $\tilde{B}_\theta = -\partial\psi/\partial r$  and  $\tilde{B}_r = im\tilde{\psi}/r$  with the boundary condition at the limiter such that  $\tilde{B}_r|_{coil} = 0$ , which should hold for rapidly oscillating modes that cannot penetrate the conducting limiters. Note that for the 2/2 mode,  $\alpha \approx 0.9$  and for the 4/3 mode  $\alpha \approx 0.7$ . Also, if the boundary condition is changed to  $\tilde{B}_r|_\infty = 0$ , then  $\alpha$  approaches unity. With the boundary condition at the limiter, at the time just before mode locking, the  $m=2, n=1$  island width is then  $W_{is} \approx 0.03$  m (Figure 5). At that time the input power was 4.2 MW and including the other quantities from a kinetically constrained equilibrium calculation using the EFIT code [24], the change in stored energy is predicted from Eq. 1 to be  $\Delta W \approx 50$  kJ. Unfortunately, the comparison with the experiment is complicated by the fact that the plasma is not in steady state and there are no similar low density ELM-free discharges without large MHD modes. Nonetheless, this calculation suggests that if there had not been a mode degrading confinement, the peak stored energy would have reached 250 kJ. The closest discharge to these conditions without a large MHD mode was in EDA H-mode and had  $\bar{n}_e = 3.5 \times 10^{20} \text{ m}^{-3}$  with nearly the same input power and a stored energy of 230 kJ. Since ELM-free H-modes generally transiently reach higher confinement than EDA H-modes, the estimated change in stored energy due to the mode is larger than previous cases but not unreasonable.

## 5. Comparison with MHD stability theory and NTM scalings

Since these moderate and large amplitude MHD modes are observed at high  $\beta$  and low collisionality, the MHD stability of one of the largest modes was calculated with the MARS code [10] and compared to separate numerical calculations to determine its proximity to marginal stability for resistive tearing modes. In addition, the operational space of the high  $\beta$  discharges has been compared with scalings from other tokamaks for the onset of NTMs.

### 5.1 MHD stability calculations compared with measurements

Resistive MHD stability was analyzed with the MARS code and with separate numerical calculations at 0.77 s for the discharge shown in Figures 1, 3a, and 4 – 6 using a kinetically constrained EFIT equilibrium. Numerical solutions of a modified Eq. 3 with a wall at the limiter radius of  $r_{coil} = 1.25a$  and with a flux surface averaged current density profile taken

from MARS, indicate that a cylindrical equivalent tearing instability index defined by the jump in the radial derivative of the perturbed poloidal flux across the rational surface  $r_s$  [25]  $\Delta'_{m,n} = (d\tilde{\psi}/dr)/\tilde{\psi}|_{r_s^+} - (d\tilde{\psi}/dr)/\tilde{\psi}|_{r_s^-} \approx 0$  for  $m=2, n=1$ . Since there are large uncertainties in the equilibrium, because there are no internal magnetic field measurements, the 2/1 mode may be marginally stable or unstable within the error bars. However, the calculated  $r_s \Delta'_{m,n} \sim 6$  was clearly unstable for the  $m=2, n=2$  mode. For all other modes checked including the 3/1, 3/2, 4/1, 4/2, 3/3, 4/3, and 4/4, the calculated  $\Delta'_{m,n}$  were substantially less than zero and so were stable. In the MARS calculations, an  $n=1$  ideal internal kink mode was found to be weakly unstable in the core. Since  $q(0) < 1$ , it is dominated by the  $m=1$  poloidal harmonic with smaller  $m=2, 3$ , and 4 sidebands. As in the separate numerical  $\Delta'$  calculations, an  $n=2$  tearing mode was also unstable at  $q=1$  with a dominant  $m=2$  poloidal harmonic, with little or no sidebands. A dominant  $m=2, n=1$  mode, as observed on the magnetic signals in the experiment, was not found in the MARS calculations, even when the resistivity profile was artificially increased by three orders of magnitude to effectively eliminate the stabilizing effect of the favorable average curvature term [26,27] in the code. These results indicate that, neglecting uncertainties in the calculated equilibrium, the observed  $m=2, n=1$  mode would be an NTM. However, given the uncertainties in the equilibrium, it is not clear whether the observed 2/1 mode is a classical or neoclassical tearing mode.

Figure 6 shows channels 2 through 8 of the ECE  $T_e$  signals together with a magnetic pick-up coil signal. A large oscillation is observed on the ECE channels from the center to near the edge at the outboard midplane and the innermost 7 channels are in phase while there is a phase inversion on the outermost 8<sup>th</sup> channel. So, the  $q=2$  surface appears to be between the 7<sup>th</sup> and 8<sup>th</sup> channels. However, EFIT, using external magnetic measurements and kinetic profiles, placed the  $q=2$  surface about 5 mm inside channel 7, which is within the uncertainties. Since the ECE measurements show no phase inversion across the  $q=1$  surface, this indicates that there is no reconnection at the  $q=1$  surface. However, the clear phase inversion near the  $q=2$  surface, between channels 7 and 8, indicates that the  $m=2$  mode is a tearing mode [28]. The absence of reconnection at the  $q=1$  surface may support the theory that differential rotation can suppress reconnection [29].

Calculations of the displacement at the  $q=1$  surface due to an  $m=2, n=1$  tearing mode in the presence of differential rotation between the two rational surfaces [27,29,30] indicate that, for an equilibrium close to being ideal unstable to the 1/1 mode, the 1/1 displacement due to the 2/1 mode can be significantly larger than the 2/1 island itself. This effect combined

with the fact that the temperature gradient is somewhat larger at the  $q=1$  surface than at the  $q=2$  surface could explain why the core oscillations are larger than the oscillations near  $q=2$  on the ECE signals, even though the 2/1 is the dominant mode on the magnetic signals. In addition, while a weak 2/2 mode is visible on the autopower spectrum of the magnetic signals (Figure 3a), no 1/1 mode is visible. The explanation could be that the 2/2 mode is a tearing mode, as found by MARS, with a relatively weak radial decay ( $\propto 1/r^3$ ) while the 1/1 displacement is an ideal kink with its typical “top hat” radial structure [22,31] that provides no significant 1/1 component of  $\tilde{B}$  at the wall. Assuming a  $1/r^3$  dependence, the 2/2 mode amplitude at the  $q=1$  surface is about 15 times lower than the 2/1 mode amplitude at the  $q=2$  surface, based on the magnetic measurements, and so the 2/2 island width would be less than 5 mm and would not be measurable on the ECE signals. Thus, the dominant  $m=2, n=1$  tearing mode on the magnetic coils appears to drive the  $m=1, n=1$  and nonlinearly the  $m=4, n=2$  harmonics and coexists with a separate  $m=2, n=2$  tearing mode.

### 5.2 Comparison with NTM theory and scalings

The neoclassical bootstrap term of the modified Rutherford equation for the time evolution of a tearing mode island width is proportional to the local quantity  $-\beta_p L_q/L_p$  [4], where the local  $\beta_p = 2\mu_0(n_i T_i + n_e T_e) / B_\theta^2$  and  $L_x = X/(dX/dr)$  is the local scale length at the mode rational surface [5]. Figure 5 shows the ratio  $-\beta_p L_q/L_T$  as a function of time during one of the discharges with rapidly growing  $m=4, n=3$  and  $m=2, n=1$  modes, where the pressure gradient has been approximated by the temperature gradient for a flat density profile. This parameter increases by nearly a factor of two over this time range as the  $m=4, n=3$  and  $m=2, n=1$  island widths, calculated from magnetic field measurements at the wall using Eq. 2, increase substantially. While the uncertainties are large, this does suggest that the neoclassical bootstrap term may be playing a role in the increasing island widths of these modes.

The high  $\beta$  operational space so far obtained on C-Mod is shown in Figure 7 using global scalings for the onset of NTMs at  $q=1.5$  and  $q=2$  from other tokamaks [7,9]. The scalings plot  $\beta_N/\rho_{*i}$  and  $\beta_N/\rho_{*i}^{1.3}$  versus the collisionality  $\nu \equiv \nu_i/(\varepsilon\omega_{*e})$ , where  $\rho_{*i} = v_{ti}/(\omega_{ci} a)$ ,  $v_{ti}$  is the ion thermal velocity,  $\omega_{ci}$  is the ion cyclotron frequency,  $a$  is the minor radius,  $\nu_i$  is the ion collision frequency,  $\varepsilon = r_s/R$ , and  $\omega_{*e}$  is the electron diamagnetic drift frequency calculated at the mode rational surface. The diamonds correspond to the five discharges with moderate to large MHD activity while the open circles correspond to discharges that did not have large MHD activity. Relative to the other high  $\beta$  points, the diamonds are some of the closest

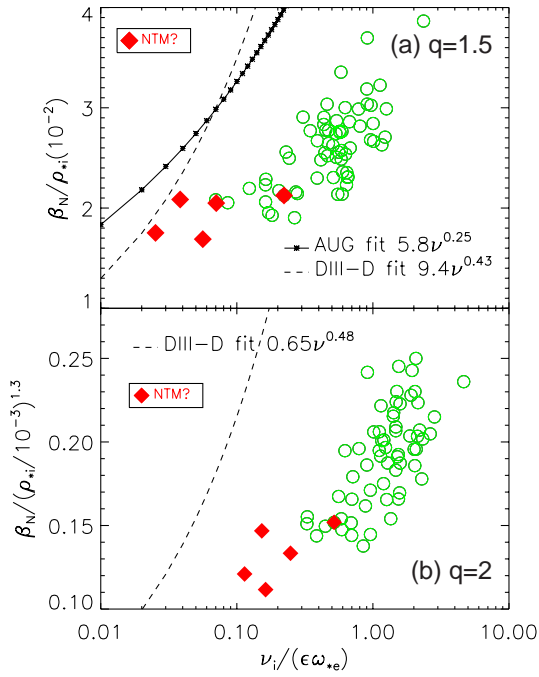


**Figure 7.** High  $\beta$  operational space for Alcator C-Mod at (a)  $q=1.5$  and (b)  $q=2$ . The diamonds correspond to the discharges with moderate to large MHD activity. The dashed lines are fits to the onset of NTM's in DIII-D and the solid line with asterisks is a fit to ASDEX-Upgrade NTM's at  $q=1.5$ .

A detailed analysis of all of the high  $\beta$  discharges from the 2000 campaign on Alcator C-Mod has found five discharges with moderate to large amplitude, low  $m, n$  MHD modes that appear to limit  $\beta$  at low collisionality. Large sawteeth are present and may provide seed islands for the growth of NTMs. In two cases, large  $m=2, n=1$  tearing modes are present that couple across the plasma to large  $m=1, n=1$  ideal internal kinks, which lock to the wall dragging down the plasma ion rotation in the core and eventually lead to disruptions. However, the C-Mod data lie about a factor of three below the  $q=2$  NTM boundary on DIII-D. In one such case, the MHD stability was calculated with the MARS code and with separate numerical  $\Delta'$  calculations and while a  $2/2$  mode was found unstable, the  $2/1$  mode was near marginal stability. The absence of a  $2/1$  mode in the MARS calculations even when the resistivity was artificially increased to reduce stabilizing effects in the code together with the particularly large amplitude of the mode observed in the experiment suggest that it could be an NTM. Uncertainties in the equilibrium, however, make it difficult to determine conclusively if these modes are classical resistive or neoclassical tearing modes. In the

points to the global scalings for the onset of NTM's observed on DIII-D [7,9] and ASDEX-Upgrade [7]. While the scaling for  $q=1.5$  is closest to some of the C-Mod points, only one discharge had an  $m=3, n=2$  mode and it had relatively high collisionality. The DIII-D scaling for the onset of NTM's at  $q=2$  is much further from the C-Mod data, which are a factor of three or more below the scaling. The diamonds have  $\nu < 0.52$ , which is close to the value of 0.3 below which neoclassical effects are expected to become important theoretically [2]. Given the uncertainties in the theory and the experimental measurements, it is possible that at least the largest of these modes are NTM's.

## 6. Conclusions

upcoming experiments, C-Mod will attempt to extend operations to lower  $v$  and higher  $\beta_N$  in order to better test such NTM scalings.

### Acknowledgements

We would like to thank Prof. F. Porcelli for stimulating discussions, Prof. A. Bondeson for providing the MARS code, and the C-Mod team for help in obtaining these data. This work was supported by D.o.E. Coop. Agreement DE-FC02-99ER54512.

### References

- [1] Greenwald M *et al* 1999 *Phys Plasmas* **6** 1943
- [2] Wilson H R *et al* 1996 *Plasma Phys Cont Fus* **38** A149
- [3] Sauter O, Angioni C, and Lin-Liu Y R 1999 *Phys Plasmas* **6** 2834
- [4] Chang Z *et al* 1995 *Phys Rev Lett* **74** 4663
- [5] Sauter O *et al* 1997 *Phys Plasmas* **4** 1654
- [6] Chang Z *et al* 1998 *Phys Plasmas* **5** 1076
- [7] LaHaye R J *et al* 2000 *Phys Plasmas* **7** 3349
- [8] Reimerdes H, Goodman T, Pochelon A, and Sauter O 2000 *Proc. 27<sup>th</sup> EPS (Budapest)* **24B** 169
- [9] LaHaye R J, Petty C C, and Strait E J, 2000 *Bull Am Phys Soc* **45** 277
- [10] Bondeson A, Vlad G, and Lütjens H, 1992 *Phys Fluids* **4** 1889
- [11] Hutchinson I H, *et al* 1994 *Phys Plasmas* **1** 1511
- [12] Hubbard A E, Hsu T C, and O'Shea P, 1995 *PFC Report PFC/JA-95-11*
- [13] Källne E, Källne J, Marmor E S, Rice J E, 1985 *Phys. Scr* **31** 551
- [14] Rice J E *et al* 1999 *Nucl Fus* **39** 1175
- [15] Fitzpatrick R and Hender T C 1991 *Phys Fluids B* **3** 644
- [16] Sauter O *et al* 2001 *Plasma Phys Cont Fus* **43** to be published from EPS 2001 conference invited paper
- [17] Chang Z and Callen J D 1990 *Nucl Fus* **30** 219
- [18] Hutchinson I H, Rice J E, Granetz R S, and Snipes J A, 2000 *Phys Rev Lett* **84** 3330
- [19] Rice J E *et al* 1998 *Nucl Fus* **38** 75
- [20] Snipes J A, Campbell D J, Hender T C, von Hellermann M, and Weisen H 1990 *Nucl Fus* **30** 205
- [21] Yushmanov, P G *et al* 1990 *Nucl Fus* **30** 1999
- [22] Wesson John, 1997 *Tokamaks Oxford University Press Oxford UK* 333
- [23] Furth H P, Rutherford P H, and Selberg H 1973 *Phys Fluids* **16** 1054
- [24] Lao L L, St John H, Stambaugh R D, Kellman A G, and Pfeiffer W 1985 *Nucl Fus* **25** 1611
- [25] White Roscoe B, Monticello D A, Rosenbluth Marshall N, and Waddell B V 1977 *Phys Fluids* **20** 800
- [26] Glasser A H, Greene J M, and Johnson J L 1975 *Phys Fluids* **18** 875
- [27] Bussac, M N, *et al* 1976 *Plasma Phys and Cont Nucl Fus Res (Proc 6<sup>th</sup> Int Conf, Berchtesgaden) IAEA Vienna* **1** 607
- [28] Fredrickson E D *et al* 1988 *Rev Sci Instrum* **8** 1797
- [29] Fitzpatrick R, Hastie R J, Martin T J, and Roach C M 1993 *Nucl Fus* **33** 1533
- [30] Connor J W *et al* 1988 *Phys Fluids* **31** 577
- [31] Bussac M N, Pellat R, Edery D, and Soule J L 1975 *Phys Rev Lett* **35** 1638